Histol Histopathol (2017) 32: 597-607

http://www.hh.um.es

Histology and Histopathology

From Cell Biology to Tissue Engineering

Immunostaining of proinflammatory cytokines in renal cortex and medulla of rats exposed to gold nanoparticles

Haseeb A. Khan[1], Khalid E. Ibrahim[2], Ayaat Khan[3], Salman H. Alrokayan[1] and Abdullah S. Alhomida[1]

[1]Department of Biochemistry, [2]Department of Zoology, College of Science, King Saud University, Riyadh, Saudi Arabia and [3]Integral Institute of Medical Sciences and Research, Lucknow, India

Summary. Recently, gold nanoparticles (GNPs) have shown promising applications in targeted drug delivery and contrast imaging. Although *in vitro* cytotoxicity of GNPs has been thoroughly studied, there are limited data on *in vivo* toxicity of GNPs. In this study, we evaluated the effects of intraperitoneally injected 10 nm and 50 nm GNPs (5 μg/animal) on the expression of proinflammatory cytokines (IL-1β, IL-6 and TNF-α) on day 1 and day 5, post-exposure. The results of immunohistochemistry showed that both 10 nm and 50 nm GNPs induced an acute phase expression of proinflammatory cytokines in renal cortex and medulla. This proinflammatory response was comparatively more intense in renal medulla than cortex. All the three cytokines were undetectable in control cortex and medulla. In conclusion, both 10 nm and 50 nm GNPs caused an acute phase induction of proinflammatory cytokines in cortex and medulla of rat kidneys. An intense immunostaining of proinflammatory cytokines in renal medulla warrants further studies to evaluate the nephrotoxicity of GNPs to validate the safe application of GNPs for contrast imaging in renal insufficiency.

Key words: Gold nanoparticles, Proinflammatory cytokines, Immunohistochemistry, Kidney, Rats

Offprint requests to: Prof. Haseeb A. Khan PhD, FRCPath, FRSC, Department of Biochemistry, College of Science, Bldg. 5, King Saud University, P.O. Box 2455, Riyadh 1145, Saudi Arabia. e-mail: khan_haseeb@yahoo.com

DOI: 10.14670/HH-11-825

Introduction

After the advent of nanotechnology, engineered nanomaterials have shown their promising applications in a wide range of areas including cosmetics, medicine, bioremediation, paints, coatings, electronics, water treatment and food industry (Weir et al., 2012; Eswar et al., 2014; Kang et al., 2015; Tapia-Hernández et al., 2015; Zehedina et al., 2015; Nafiujjaman et al., 2015; Nurunnabi et al., 2015; Zhang et al., 2016). Gold nanoparticles (GNPs), though made from chemically inert metal, exhibit altered behavior at nanoscale and have emerged as a promising tool for the controlled release and delivery of various chemical agents, including anticancer drugs (Craig et al., 2012), antibiotics (Perni and Prokopovich, 2014), antibodies (Cabezón et al., 2015), vaccines (Chiodo and Marradi, 2015), proteins (Ryou et al., 2014), and nucleic acids (Ekin et al., 2014). Wen et al. (2013) designed gadolium-loaded dendrimer-entrapped GNPs for dual mode computed tomography (CT) and magnetic resonance imaging (MRI) of the bladder, heart, liver, and kidney of rat or mouse within a short time frame (45 min) and their clearance from the major organs within 24 h. Alric et al. (2013) functionalized GNPs with dithiopolyamino-carboxylate (DTPA) for imaging applications so that the gold core and a DTPA shell can be established by X-ray imaging (due to X-ray absorption of the gold core) and by MRI as the DTPA shell was designed to immobilize the paramagnetic gadolinium ions. Recently, water-dispersible ultrasmall dopamine-coated GNPs showed a much longer circulation time and a larger CT attenuation coefficient than iohexol, suggesting their considerable

potential for future application in CT imaging (Yu et al., 2016).

Because of the large scale synthesis and widespread applications of nanomaterials, there is a growing trend towards understanding the harmful effects of nanomaterials to ensure their safe application and sustainable remediation. Since nanomedicine and nanotoxicology are two sides of the same coin, the worth of this coin depends on its prudent use (Khan and Shanker, 2015). The promise of GNPs for several biological applications has led to strong interest in understanding their interaction with biological systems (Alkilany and Murphy, 2010). Although the primary site of GNP accumulation is liver, there is a lack of *in vivo* and *in vitro* toxicity information to allow correlations between the findings to be made (Johnston et al., 2010). It is important to note that *in vitro* toxicity using cell lines would not necessarily reflect the *in vivo* toxicity as seen in animals because the former setup lacks in the immune response and microenvironment, being the features of live organs. Morais et al. (2012) studied the biodistribution of GNPs (20 nm) with different surface coatings and concluded that GNPs are rapidly distributed in the body while the liver is the preferential accumulation organ with most GNPs trapped in Kupffer cells, hepatocytes and endosomes. Buzulukov et al. (2014) evaluated the bioaccumulation of GNPs (35 nm) after their intragastric administration to rats at a dose of 100 µg/kg for 2 weeks. Their results showed that GNPs were detected in all biological samples studied (liver, kidney, spleen, heart, gonads brain, and blood), the highest specific weight and content of GNP being found in kidneys of animals (Buzulukov et al., 2014). Intraperitoneal administration of small and medium sized GNPs produced transient increases in pro-inflammatory cytokines expression in rat liver (Khan et al., 2013a, 2016). Considering the important emerging role of GNPs in contrast imaging, it would be intriguing to examine the effect of GNPs on the major excretory organ, kidney. This immunohistochemical study aimed to determine the expression of proinflammatory cytokines including IL-1β, IL-6 and TNF-α in kidney cortex and medulla of rats exposed to 10 nm and 50 nm GNPs.

Materials and methods

Animals and treatment groups

Adult male Wistar rats (body weight 220±10 g) were received from the Laboratory Animal Centre, College of Pharmacy, King Saud University, Riyadh, Saudi Arabia. The animals were maintained in a temperature- and humidity-controlled room with 12 h light/dark cycles and with free access to standard laboratory food and drinking water. The rats were divided randomly into 5 study groups of 5 animals in each group. One group served as control and received vehicle only. Two groups were treated with 10 nm GNPs, for 1 day or daily for 5 days. The remaining two groups received 50 nm GNPs, for 1 day or daily for 5 days.

Dosing of gold nanoparticles

Commercially available GNPs of 10 nm diameter (MKN-Au-010 of concentration 0.01% Au) and 50 nm (MKN-Au-050 of concentration 0.01% Au) were purchased from MK Impex Corp., Ontario, Canada. Doses of 50 µl of 10 nm and 50 nm GNPs in aqueous solution were intraperitoneally injected to animals, daily for 1 or 5 days. This dose regimen was approximately equivalent to 5 µg/animal of 10 nm GNP (number of particles, 2.85×10^{11}) or 50 nm GNP (number of particles, 2.25×10^{9}) and did not affect the animal bodyweight as compared to control group.

The rats were sacrificed 24 h after the last injection of GNPs. The specimens of kidneys were isolated and immediately fixed in 10% neutral buffered formalin for 72 h. All experiments were conducted in accordance with guidelines approved by our Institutional Animal Care and Use Committee.

Immunohistochemistry

The fixed kidney specimens were processed overnight for washing, dehydration, clearing and impregnation using an automatic tissue processor (Sakura, Japan). The specimens were embedded in paraffin blocks using embedding station (Sakura, Japan) and sections of 4 micron thickness were cut using a rotary microtome (Leica-RM2245, Germany) and mounted on super frosted slides for immunostaining.

The paraffin-embedded tissue sections were deparaffinized by passing them through xylene, ethanol (100%, 95%, 80%, sequentially) and distilled water. Then the sections were primed for antigen retrieval by microwave heating for 5 min in citrate buffer solution (pH 6.0). This treatment unmasks the antigenic sites and makes the sections ready for immunostaining protocol using Expose Mouse and Rabbit Specific HRP/DAB Detection IHC kit (Abcam).

For immunostaining, the sections were incubated with 3% hydrogen peroxide for 10 min to block the endogenous peroxidase activity followed by incubation with 0.1% protein blocking solution for 10 minutes to prevent nonspecific background staining. The phosphate buffer saline (PBS, pH 7.4) washings were performed three times after each step. The unlabeled primary antibody with optimal dilution (IL-1β 1:500, IL-6 1:400, TNF-α 1:100) was applied and incubated for 1 h at room temperature followed by PBS washing and incubation with complement for 30 min. After washing steps, the sections were incubated with horseradish peroxidase (HRP) conjugate for 30 min followed by washing and incubation with the DAB substrate for 10 min. After a final rinse with distilled water, the sections were counterstained with Mayer's Hematoxylin for 2 min for light microscopic observation. For semi-quantitative

analysis, we used low magnification (×200) images to cover a larger observational area. The intensity of immunostaining was graded on a 0 (no staining) to 5 (highest intensity and maximum area) scale.

Statistics

The data were analyzed by one-way analysis of variance (ANOVA) followed by Dunnett's multiple comparison test using SPSS statistical package. P values less than 0.05 were considered as statistically significant.

Results

The immunohistochemistry of renal cortex did not show any IL-1β specific staining in control rats, whereas administration of 10 nm and 50 nm GNPs induced IL-1β expression on day 1 that persisted on day 5 (Fig. 1). The immunostaining for IL-6 was absent in the renal cortex of control animals. In GNP treated groups, although only few animals showed IL-6 specific immunostaining in renal cortex on day 1, their frequency and intensity increased on day 5 (Fig. 2). TNF-α immunostaining was absent in the renal cortex of all the animals except one animal in 50 nm GNP group that showed light staining on day 1 and day 5 (Fig. 3).

The renal medulla of control animals did not show any IL-1β immunostaining (Fig. 4). Both 10 nm and 50 nm GNPs caused intense immunostaining of IL-1β in renal cortex on day 1 that was slightly reduced on day 5 in the former group but increased in the latter group (Fig. 4). The immunostaining for IL-6 was absent in control renal medulla, whereas both 10 nm and 50 nm GNPs produced intense immunostaining for IL-6 on day 1 that was reduced on day 5 (Fig. 5). The expression of TNF-α was absent in the renal medulla of control as well as 10 nm GNP group (except one animal which showed mild immunostaining on day 1) although 50 nm GNPs caused intense immunostaining for TNF-α on day 1 that subsided on day 5 (Fig. 6).

The results of semi-quantitative analysis showed a significant and dose dependent increase in IL-1β immunostaining in renal cortex on day 1 post-dosing of 50 nm GNPs, that was marginally reduced on day 5 (ANOVA F=4.92, P=0.006) (Fig. 1, lower panel). Although both 10 nm and 50 nm GNPs increased the expression of IL-6 in cortex, it was significant only on day 5 following exposure of 10 nm GNPs (ANOVA F=3.56, P=0.024) (Fig. 2, lower panel). The expression of TNF-α was not induced by GNPs in the renal cortex of rats (ANVOA F=0.75, P=0.570) (Fig. 3, lower panel). In the medulla of rat kidneys, both 10 nm and 50 nm GNPs significantly increased the IL-1β expression on day 1 that was reduced on day 5 in the case of smaller GNPs but increased for larger GNPs (ANOVA F=8.37, P=0.001) (Fig. 4, lower panel). Administration of 10 nm GNPs caused a highly significant increase in IL-6 immunostaining on day 1 that was reduced to almost half on day 5 (ANOVA F=31.84, P=0.001). In the case of 50 nm GNPs, the significant increase in IL-6 expression on day 1 persisted until day 5 (Fig. 5, lower panel). Although 10 nm GNPs had no significant impact on TNF-α expression, 50 nm GNPs significantly increased TNF-α immunostaining that subsided on day 5 (ANOVA F=14.20, P=0.001) (Fig. 6, lower panel).

Discussion

The results showed that administration of GNPs produced comparatively milder immunostaining of IL-1β and IL-6 in renal cortex (Figs. 1, 2) than medulla (Figs. 4, 5). TNF-α immunostaining was almost undetectable in renal cortex of GNPs treated rats with either doses (Fig. 3) whereas 50 nm GNPs caused significant immunostaining of TNF-α in renal medulla (Fig. 6, Table 1). Another important finding was an increased induction of IL-6 by smaller GNPs (10 nm) whereas larger GNPs (50 nm) were more potent in inducing the expressions of IL-1β and TNF-α. All the three cytokines were undetectable in control cortex or medulla using immunohistochemistry. Previously, real-time PCR analysis showed that 10 nm GNPs did not affect the IL-1β, IL-6 and TNF-α mRNA in renal cortex of rats, but 50 nm GNPs induced the expression of IL-6 and TNF-α on day 1 that subsided on day 5 (Khan et al., 2013b). A comparatively milder induction of some of the proinflammatory cytokines expression by 10 nm GNPs may be attributed to faster renal clearance of small sized GNPs. Despite comparatively smaller pore size (8 nm) of glomerular basement membrane, the urinary excretion of 20 nm GNPs has been linked to neutral or small charges on GNPs, which help in counteracting repulsive forces and enabling them to pass through the filtration barrier (Balasubramanian et al., 2010). The accumulation of GNPs in rat liver after 24 h of the intravenous injection was reported to be in the range from 91.9% to 96.9% for 5 nm, 18 nm, 80 nm and 200 nm GNPs, whereas their hepato-biliary clearance showed an inverse linear relationship to the GNP size over the range of 5 nm to 200 nm (Hirn et al., 2011).

Particle size plays a key role in immunoreactivity because of the differential deposition of complement proteins that is affected by the size of NPs. Recently we have shown that a complement system plays an important role in uptake and clearance of nanoparticles as well as the modulation of proinflammatory immune response (Pondman et al., 2015). Lee et al. (2015) studied the role of surface charge on blood kinetics, organ distribution and elimination pattern of intravenously injected GNPs (15 nm, 1 mg/kg) in mice. They injected PEG-coated GNPs (neutral) as well as carboxyl (negative charge) or amino (positive charge) groups conjugated GNPs into mice and the concentration of Au was measured in different organs at different time points from 30 min to 6 months post-injection. The preferential organ distribution was as follows: neutral GNPs for mesenteric lymph node, kidney, brain and testis; negatively charged GNPs for liver; positively

charged GNPs for spleen, lung and heart (Lee et al., 2015). Zhang et al. (2014) coated bovine serum albumin (BSA) on the surface of three types of gold nanomaterials including gold nanocluster (GNC), gold nanorod (GNR) and gold nanosphere (GNS) to increase their plasma stability while investigating their

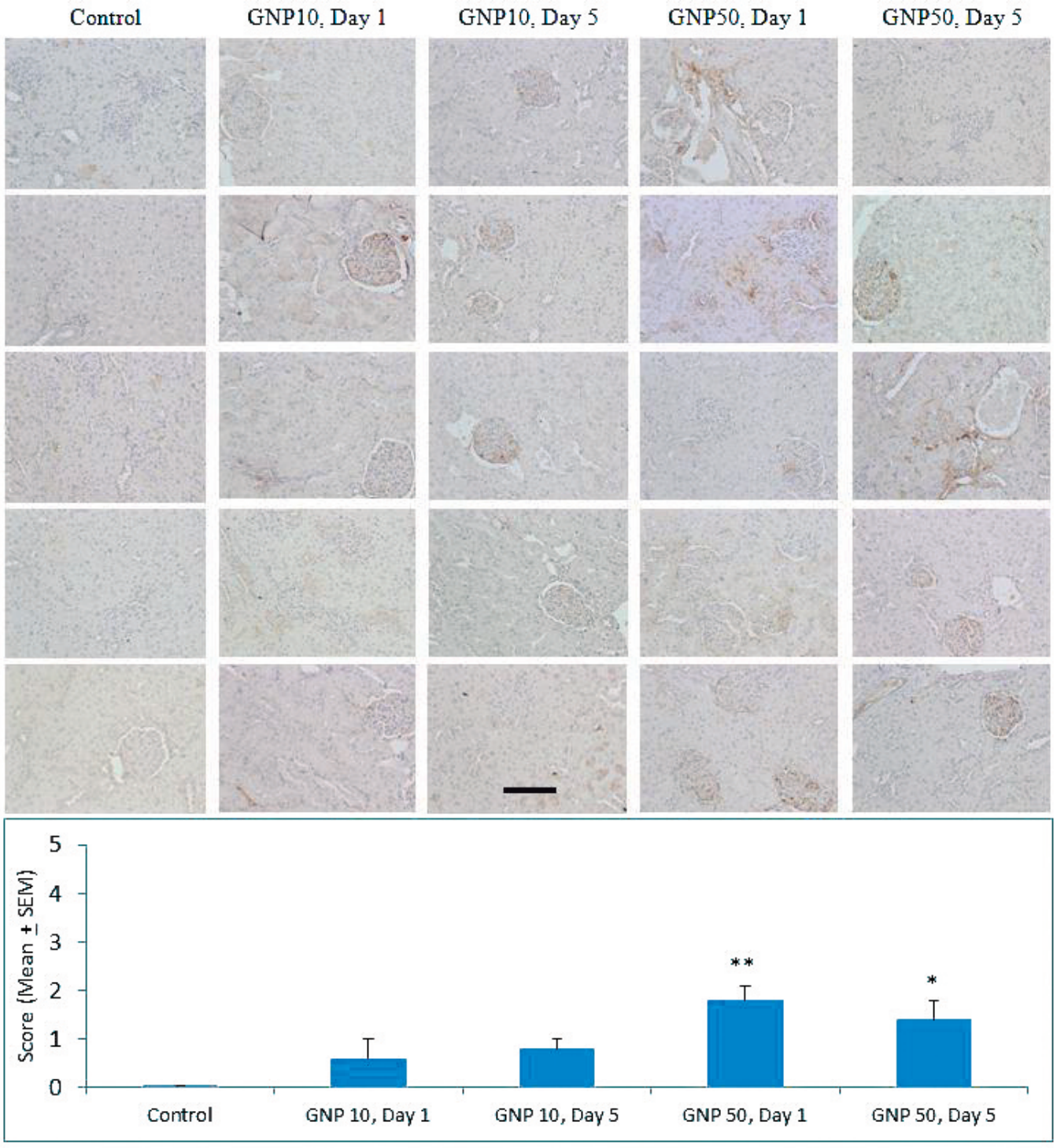

Fig. 1. Immunostaining of IL-1β in renal cortex of rats in different treatment groups. Images from top to bottom represent different animals in respective groups. Lower panel bar graph shows the semi-quantitative analysis of immunostaining as the average 5 animals in each group. *P<0.05 and **P<0.01 versus control group using Dunnett's multiple comparison test. Scale bar: 50 μm.

biodistribution and toxicities in mice. After intravenous administration of the above gold nanomaterials with an equal content of gold element at 0.5 mg/kg in mice, huge differences were observed in kidney accumulation of GNC and hydrolyzed GNC with their sizes at 7.1 and 3.2 nm. Moreover, GNR and GNS of relative large size

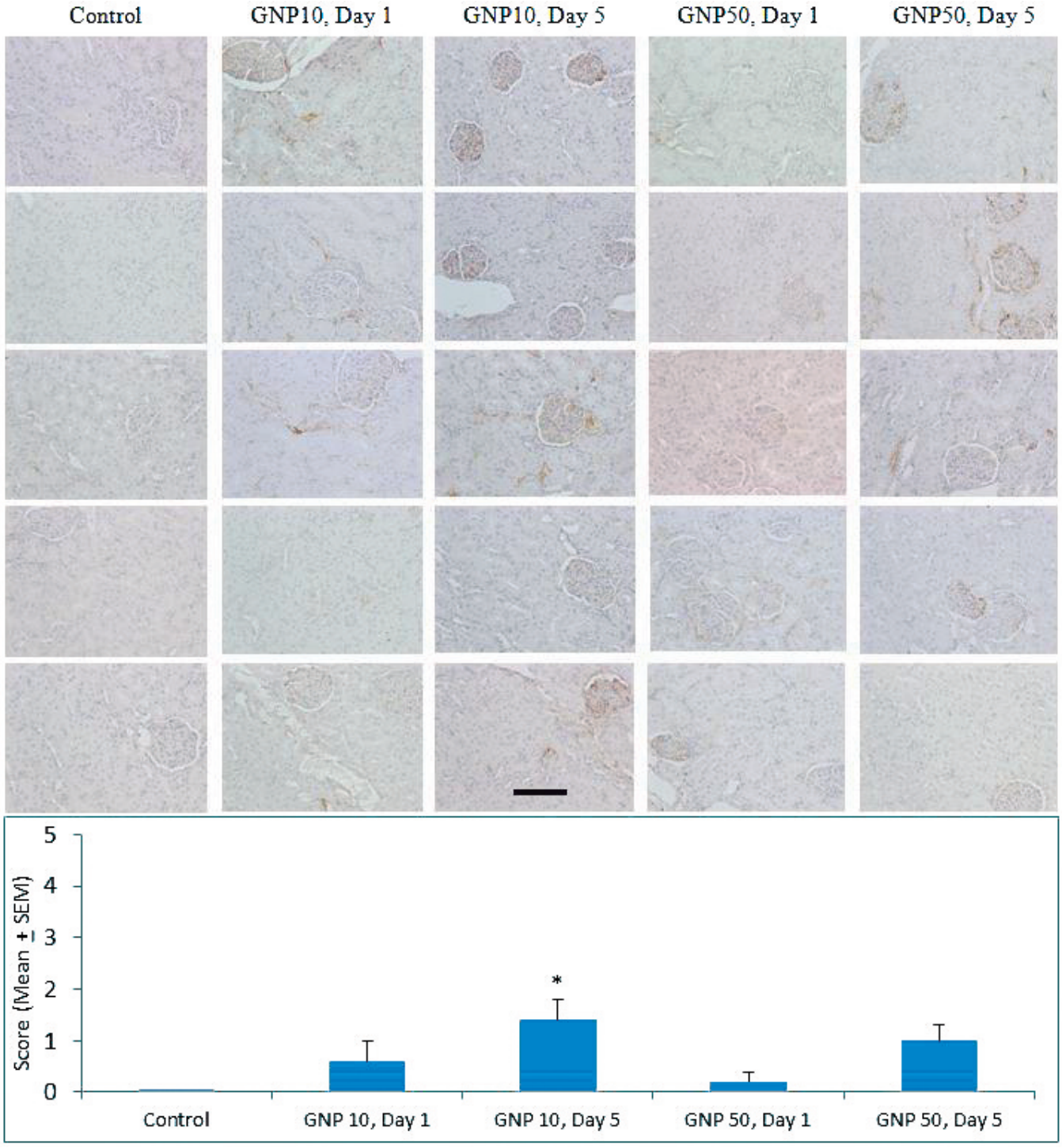

Fig. 2. Immunostaining of IL-6 in renal cortex of rats. Images from top to bottom represent different animals in respective groups. Lower panel bar graph shows the semi-quantitative analysis of immunostaining as the average of 5 animals in each group. *P<0.05 versus control group using Dunnett's multiple comparison test. Scale bar: 50 μm.

preferred to accumulate in liver and spleen, whereas GNC of relative small size tended to accumulate in liver and kidney (Zhang et al., 2014). The presence of GNPs in liver persisted for as long as 28 days whereas their accumulation in kidney was eliminated in a short time (Zhang et al., 2014). Recently, Naz et al. (2016) have

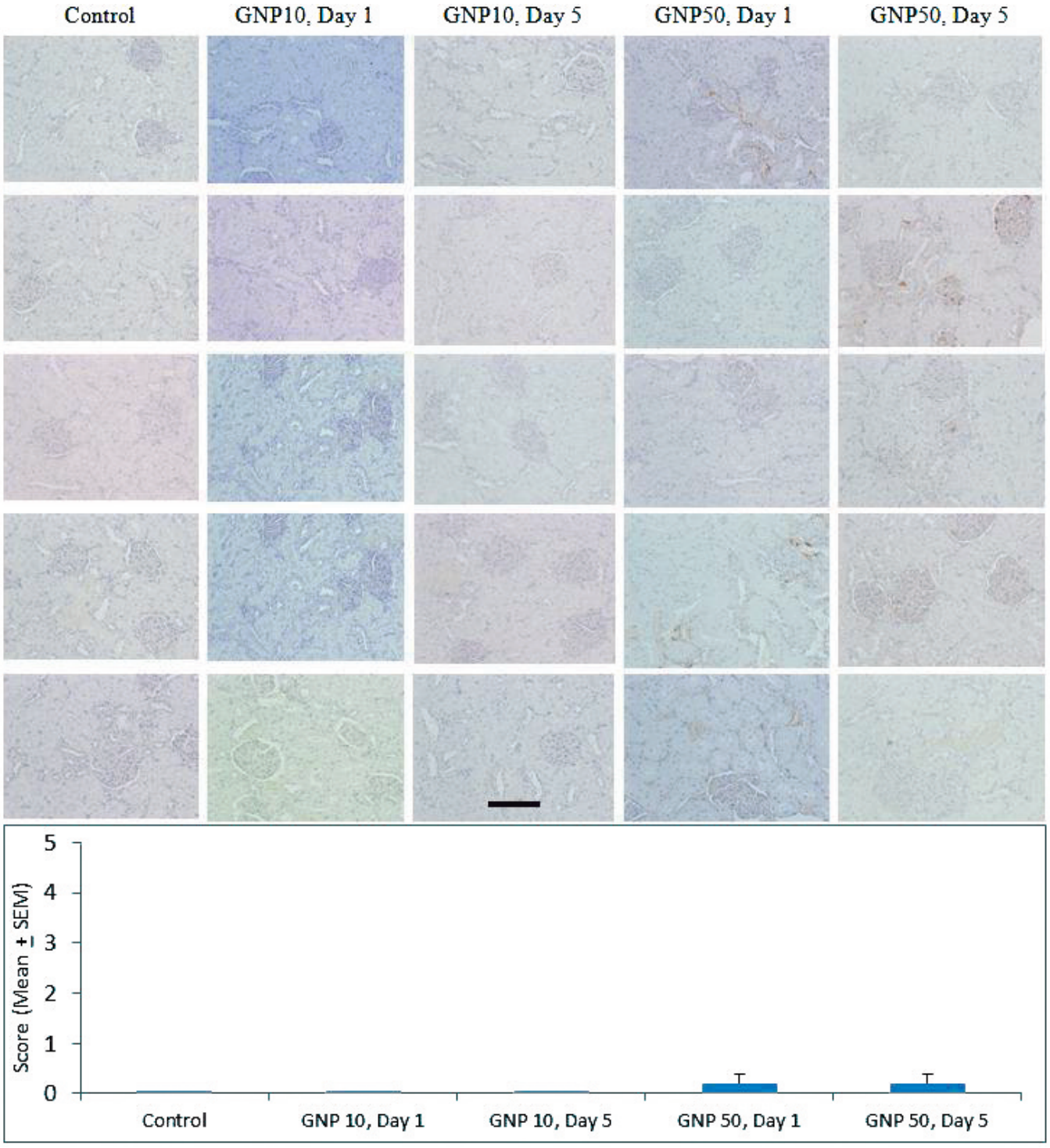

Fig. 3. Immunostaining of TNF-α in renal cortex of rats. Images from top to bottom represent different animals in respective groups. Lower panel bar graph shows the semi-quantitative analysis of immunostaining as the average of 5 animals in each group. Scale bar: 50 μm.

shown that ultrafine GNPs (2-10 nm) are predominantly excreted in urine without any systemic toxicity following intravenous administration and are safe for use in drug delivery systems. However, the same study observed that GNPs were detectable in urine till 30 days after single injection, indicating slow excretion from the

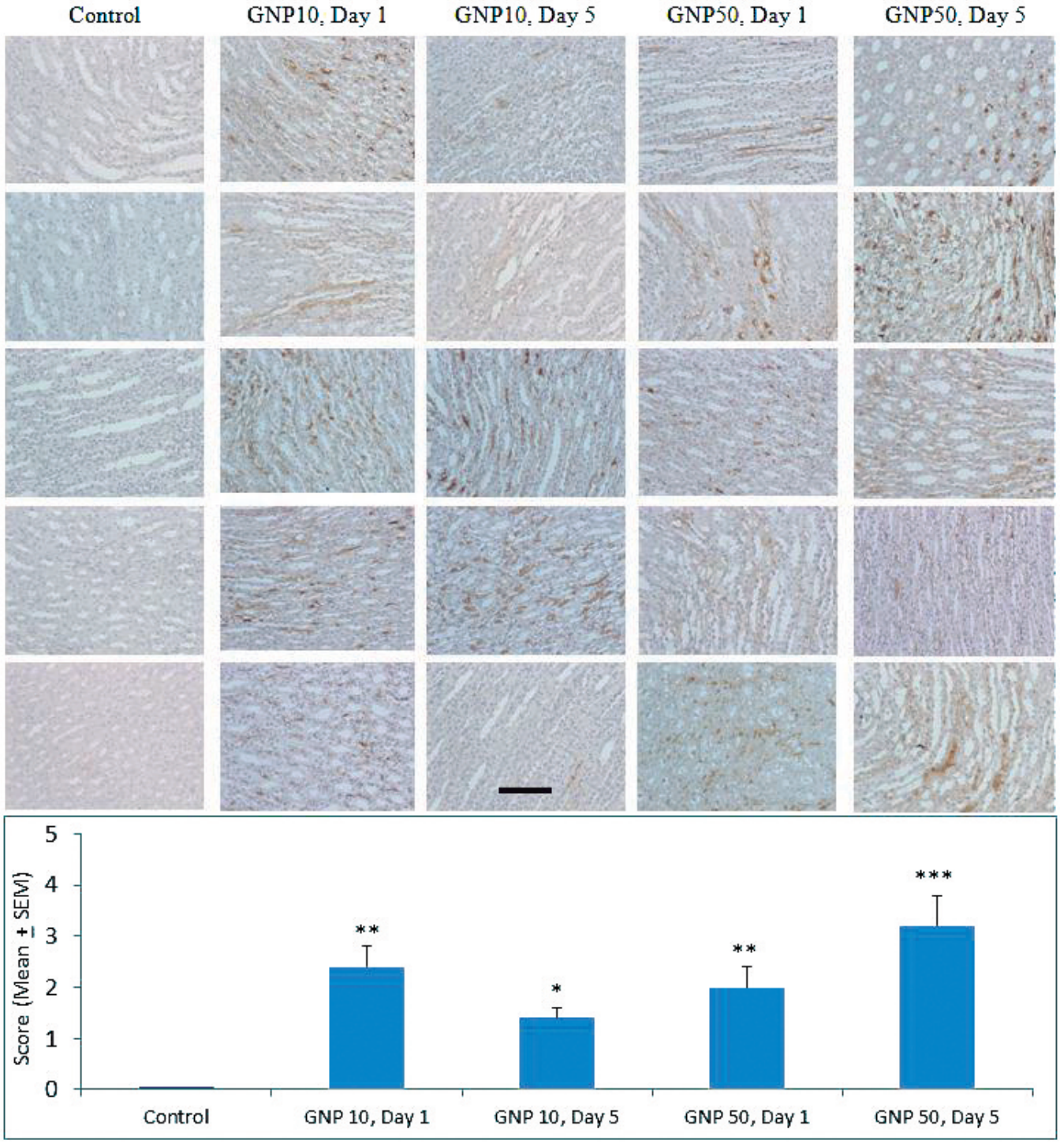

Fig. 4. Immunostaining of IL-1β in renal medulla of rats. Images from top to bottom represent different animals in respective groups. Lower panel bar graph shows the semi-quantitative analysis of immunostaining as the average of 5 animals in each group. *P<0.05, **P<0.01 and ***P<0.001 versus control group using Dunnett's multiple comparison test. Scale bar: 50 μm.

body.

Induction of cytokines is a part of natural immunological defense against foreign antigens. In some cases, a declining trend of proinflammatory cytokines expression on day 5 indicated that 10 nm and 50 nm GNPs do not exert sustained immunotoxicity. Based on

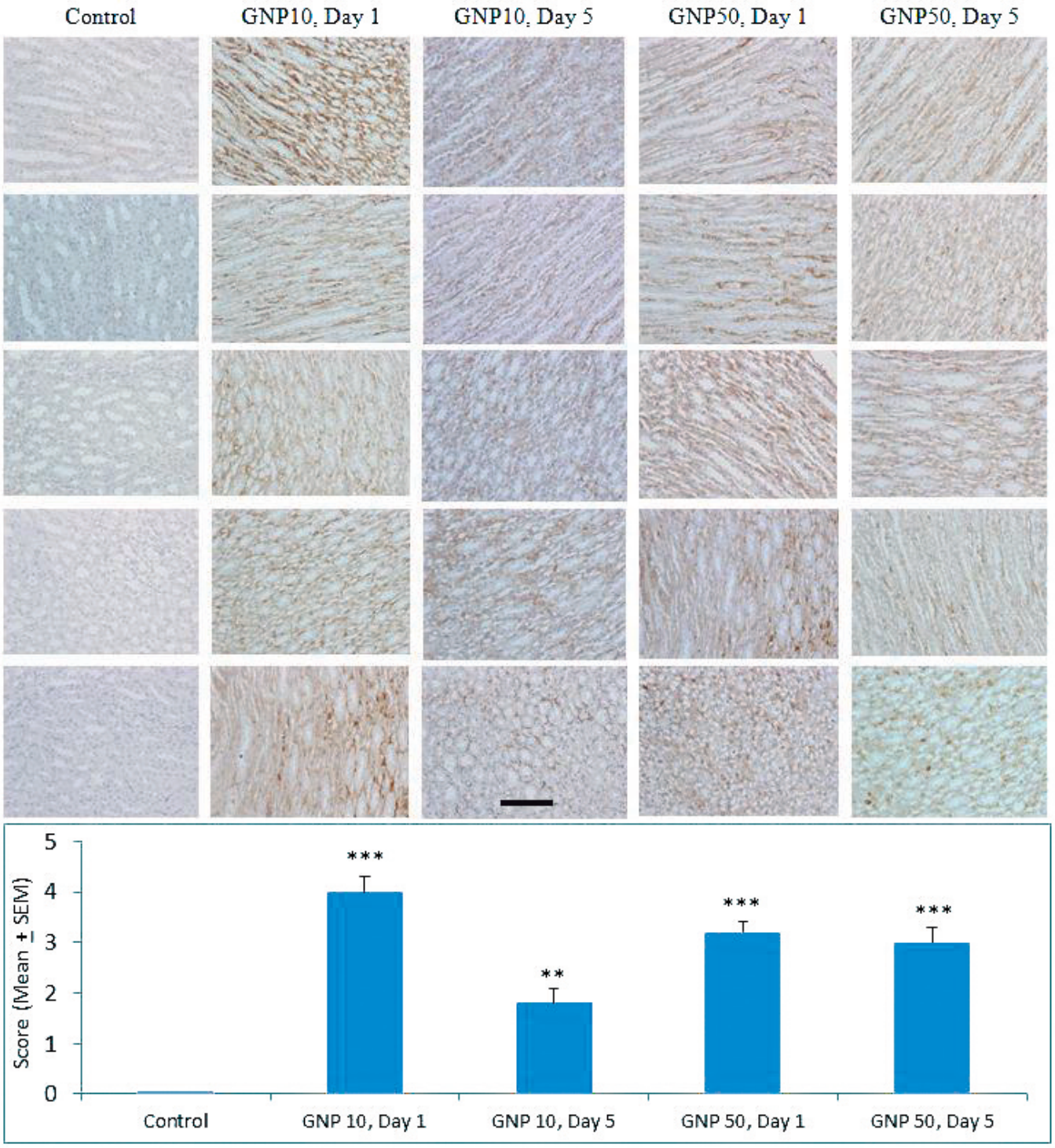

Fig. 5. Immunostaining of IL-6 in renal medulla of rats. Images from top to bottom represent different animals in respective groups. Lower panel bar graph shows the semi-quantitative analysis of immunostaining as the average of 5 animals in each group. **P<0.01 and ***P<0.001 versus control group using Dunnett's multiple comparison test. Scale bar: 50 μm.

pathology, immune response, and blood biochemistry, it has been shown that PEG-coated GNPs of different sizes (4.8-46.6 nm) did not cause any damage to spleen and kidneys (Zhang et al., 2012). Histopathological examination of 22 organs showed no evidence of organ injury or organ dysfunction following short term (14

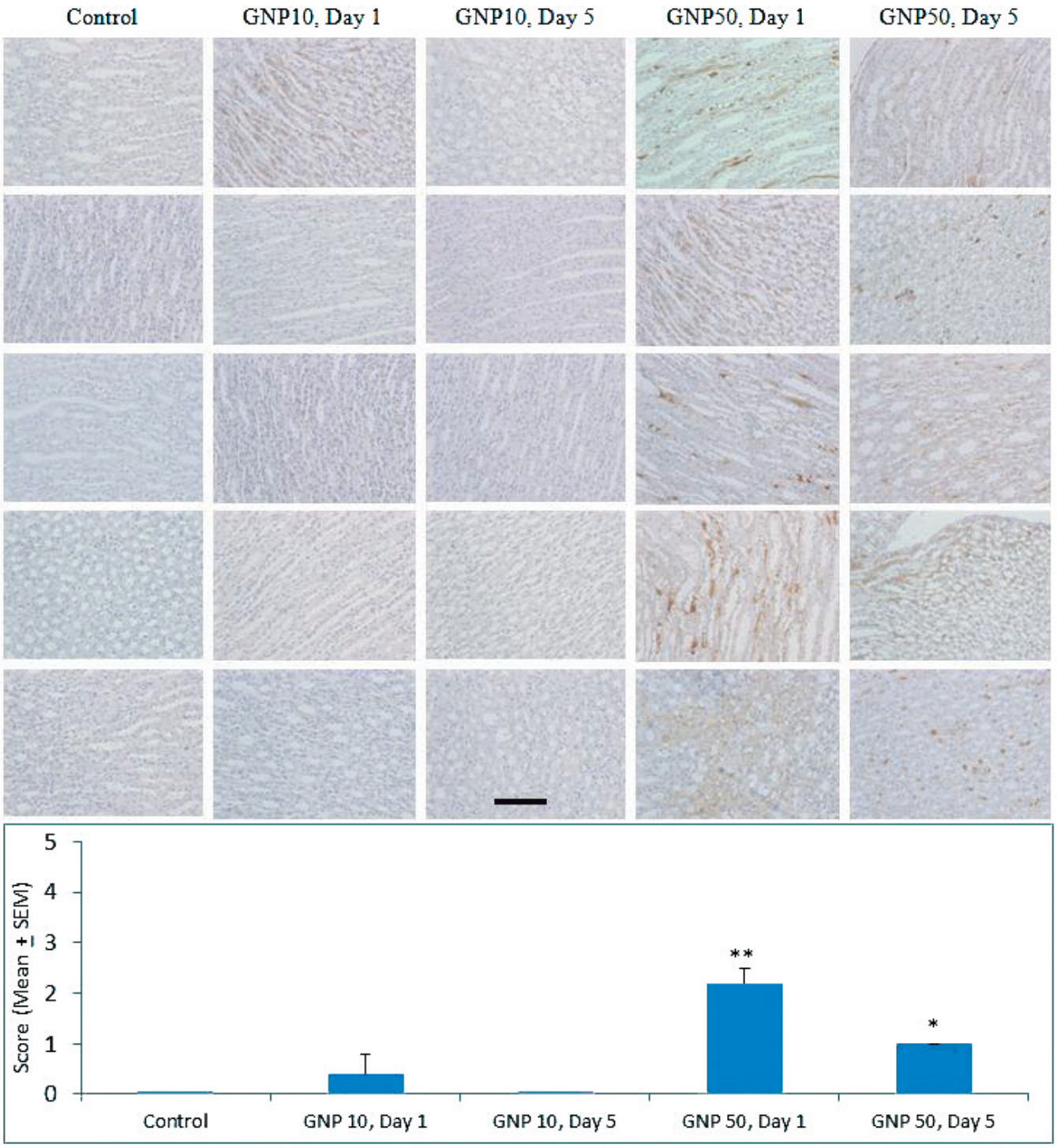

Fig. 6. Immunostaining of TNF-α in renal medulla of rats. Images from top to bottom represent different animals in respective groups. Lower panel bar graph shows the semi-quantitative analysis of immunostaining as the average of 5 animals in each group. *P<0.05 and **P<0.01 versus control group using Dunnett's multiple comparison test. Scale bar: 50 μm.

days) or long-term (78 days) exposure of dendrimer-based GNPs in mice (Kasturirangan et al., 2013). However, if the proinflammatory cascade remains effective for a longer duration it may lead to cellular injury via excessive generation of reactive oxygen species (ROS). Shrivastava et al. (2016) have observed a significant increase in ROS and depletion of antioxidant enzyme status in erythrocytes and tissues of mice exposed to GNPs. Intraperitoneal injection of 10 nm and 30 nm GNP caused oxidative stress and altered the energy metabolism in liver, heart and kidneys of rats (Ferreira et al., 2015). The levels of inflammatory markers, IL-6 and nitric oxide synthase were increased in plasma following exposure to GNPs with accompanied hepatotoxicity (Shrivastava et al., 2016). Intraperitoneal injection of 10 nm diameter GNPs significantly increased liver malondialdehyde without altering glutathione levels in rat liver, on 3 and 7 days post-dosing (Khan et al., 2012). In a histopathological study, injection of 25 ppm GNPs for 14 days did not cause any renal damage in cortex and medulla whereas the higher doses (50 and 100 ppm) produced significant and dose-dependent damage to renal cortex and renal corpuscle (Ajdary et al., 2015). The renal injury was also associated with significant increases in blood urea nitrogen in the medium and high dose groups (Ajdary et al., 2015).

In conclusion, both 10 nm and 50 nm GNPs caused an acute phase induction of proinflammatory cytokines in cortex and medulla of rat kidneys. This proinflammatory response was comparatively more intense in renal medulla than cortex. In some cases, the intensity of proinflammatory cytokines expression receded on day 5. Although an acute phase induction of proinflammatory cytokines is a normal phenomenon of natural defense a sustained proinflammatory cascade may lead to cellular injury. An intense immunostaining of proinflammatory cytokines in renal medulla warrants further studies to evaluate the nephrotoxicity of GNPs in an animal model with impaired renal function to validate the safe application of GNPs for contrast imaging.

Acknowledgements. The authors would like to extend their sincere appreciation to the Deanship of Scientific Research at King Saud University for funding the Research Group No. RGP-066.

References

Ajdary M., Ghahnavieh M.Z. and Naghsh N. (2015). Sub-chronic toxicity of gold nanoparticles in male mice. Adv. Biomed. Res. 4, 67.

Alkilany A.M. and Murphy C.J. (2010). Toxicity and cellular uptake of gold nanoparticles: what we have learned so far? J. Nanopart. Res. 12, 2313-2333.

Alric C., Miladi I., Kryza D., Taleb J., Lux F., Bazzi R., Billotey C., Janier M., Perriat P., Roux S. and Tillement O. (2013). The biodistribution of gold nanoparticles designed for renal clearance. Nanoscale 5, 5930-5939.

Balasubramanian S.K., Jittiwat J., Manikandan J., Ong C.N., Yu L.E. and Ong W.Y. (2010). Biodistribution of gold nanoparticles and gene expression changes in the liver and spleen after intravenous administration in rats. Biomaterials 31, 2034-2042.

Buzulukov I.P., Arianova E.A., Demin V.F., Safenkova I.V., Gmoshinskiĭ I.V. and Tutel'ian V.A. (2014). Bioaccumulation of silver and gold nanoparticles in organs and tissues of rats by neutron activation analysis. Izv. Akad. Nauk. Ser. Biol. 3, 286-295.

Cabezón I., Manich G., Martín-Venegas R., Camins A., Pelegrí C. and Vilaplana J. (2015). Trafficking of gold nanoparticles coated with the 8D3 anti-transferrin receptor antibody at the mouse blood-brain barrier. Mol. Pharm. 12, 4137-4145.

Chiodo F. and Marradi M. (2015). Gold nanoparticles as carriers for synthetic glycoconjugate vaccines. Methods Mol. Biol. 1331, 159-171.

Craig G.E., Brown S.D., Lamprou D.A., Graham D. and Wheate N.J. (2012). Cisplatin-tethered gold nanoparticles that exhibit enhanced reproducibility, drug loading, and stability: a step closer to pharmaceutical approval? Inorg. Chem. 51, 3490-3497.

Ekin A., Karatas O.F., Culha M. and Ozen M. (2014). Designing a gold nanoparticle-based nanocarrier for microRNA transfection into the prostate and breast cancer cells. J. Gene Med. 16, 331-335.

Eswar K.A., Rouhi J., Husairi F.S., Dalvand R., Alrokayan S.A., Khan H.A., Mahmood R. and Abdullah S. (2014). Hydrothermal growth of flower-like ZnO nanostructures on porous silicon substrate. J. Mol. Struc. 1074, 140-143.

Ferreira G.K., Cardoso E., Vuolo F.S., Michels M., Zanoni E.T., Carvalho-Silva M., Gomes L.M., Dal-Pizzol F., Rezin G.T., Streck E.L. and Paula M.M. (2015). Gold nanoparticles alter parameters of oxidative stress and energy metabolism in organs of adult rats. Biochem. Cell. Biol. 93, 548-557.

Hirn S., Semmler-Behnke M., Schleh C., Wenk A., Lipka J., Schäffler M., Takenaka S., Möller W., Schmid G., Simon U. and Kreyling W.G. (2011). Particle size-dependent and surface charge-dependent biodistribution of gold nanoparticles after intravenous administration. Eur. J. Pharm. Biopharm. 77, 407-416.

Johnston H.J., Hutchison G., Christensen F.M., Peters S., Hankin S. and Stone V. (2010). A review of the *in vivo* and *in vitro* toxicity of silver and gold particulates: particle attributes and biological mechanisms responsible for the observed toxicity. Crit. Rev. Toxicol. 40, 328-346.

Kang S.H., Nafiujjaman M., Nurunnabi M., Li L., Khan H.A., Cho K.J., Huh K.M. and Lee Y. (2015). Hybrid photoactive nanomaterial composed of gold nanoparticles, pheophorbide-A and hyaluronic acid as a targeted bimodal phototherapy. Macromol. Res. 23, 474-484.

Khan H.A., Abdelhalim M.A., Al Ayed M.S. and Alhomida A.S. (2012). Effect of gold nanoparticles on glutathione and malondialdehyde levels in liver, lung and heart of rats. Saudi J. Biol. Sci. 19, 461-464.

Khan H.A., Abdelhalim M.A., Alhomida A.S. and Al Ayed M.S. (2013a). Transient increase in IL-1β, IL-6 and TNF-α gene expression in rat liver exposed to gold nanoparticles. Genet. Mol. Res. 12, 5851-5857.

Khan H.A., Abdelhalim M.A., Alhomida A.S. and Al Ayed M.S. (2013b). Effects of naked gold nanoparticles on proinflammatory cytokines mRNA expression in rat liver and kidney. Biomed. Res. Int. 2013, 590730.

Khan H.A., Ibrahim K.E., Khan A., Alrokayan S.H., Alhomida A.S., Lee Y.K. (2016). Comparative evaluation of immunohistochemistry and real-time PCR for measuring proinflammatory cytokines gene

expression in livers of rats treated with gold nanoparticles. Exp. Toxicol. Pathol. 68, 381-390.

Khan H.A. and Shanker R. (2015).Toxicity of nanomaterials. Biomed. Res. Int. 2015, 521014.

Kasturirangan V., Nair B.M., Kariapper M.T., Lesniak W.G., Tan W., Bizimungu R., Kanter P., Toth K., Buitrago S., Rustum Y.M., Hutson A., Balogh L.P. and Khan M.K. (2013). *In vivo* toxicity evaluation of gold-dendrimer composite nanodevices with different surface charges. Nanotoxicology 7, 441-451.

Lee J.K., Kim T.S., Bae J.Y., Jung A.Y., Lee S.M., Seok J.H., Roh H.S., Song C.W., Choi M.J., Jeong J., Chung B.H., Lee Y.G., Jeong J. and Cho W.S. (2015). Organ-specific distribution of gold nanoparticles by their surface functionalization. J. Appl. Toxicol. 35, 573-580.

Morais T., Soares M.E., Duarte J.A., Soares L., Maia S., Gomes P., Pereira E., Fraga S., Carmo H. and Bastos M.L. (2012). Effect of surface coating on the biodistribution profile of gold nanoparticles in the rat. Eur. J. Pharm. Biopharm. 80, 185-193.

Nafiujjaman M., Nurunnabi M., Kang S.H., Reeck G., Khan H.A. and Lee Y. (2015). Ternary graphene quantum dot-polydopamine-Mn_3O_4 nanoparticles for optical imaging guided photodynamic therapy and T1-weighted magnetic resonance imaging. J. Mater. Chem. B. 3, 5815-5823.

Naz F., Koul V., Srivastava A., Gupta Y.K. and Dinda A.K. (2016). Biokinetics of ultrafine gold nanoparticles (AuNPs) relating to redistribution and urinary excretion: a long-term *in vivo* study. J. Drug Target. 24, 720-729.

Nurunnabi M., Parvez K., Nafiujjaman M., Revuri V., Khan H.A., Feng X. and Lee Y. (2015). Bioapplication of graphene oxide derivatives: drug/gene delivery, imaging, polymeric modification, toxicology, therapeutics and challenges. RSC Adv. 5, 42141-42161.

Perni S. and Prokopovich P. (2014). Continuous release of gentamicin from gold nanocarriers. RSC Adv. 4, 51904-51910.

Pondman K.M., Pednekar L., Paudyal B., Tsolaki A.G., Kouser L., Khan H.A., Shamji M.H., Haken B.T., Stenbeck G., Sim R.B. and Kishore U. (2015). Innate immune humoral factors, C1q and factor H, with differential pattern recognition properties, alter macrophage response to carbon nanotubes. Nanomedicine 11, 2109-2118.

Ryou S.M., Yeom J.H., Kang H.J., Won M., Kim J.S., Lee B., Seong M.J., Ha N.C., Bae J. and Lee K. (2014). Gold nanoparticle-DNA aptamer composites as a universal carrier for *in vivo* delivery of biologically functional proteins. J. Control Release. 196, 287-294.

Shrivastava R., Kushwaha P., Bhutia Y.C. and Flora S. (2016). Oxidative stress induced following exposure to silver and gold nanoparticles in mice. Toxicol. Ind. Health 32, 1391-1404.

Tapia-Hernández J.A., Torres-Chávez P.I., Ramírez-Wong B., Rascón-Chu A., Plascencia-Jatomea M., Barreras-Urbina C.G., Rangel-Vázquez N.A. and Rodríguez-Félix F. (2015). Micro- and nanoparticles by electrospray: advances and applications in foods. J. Agric. Food Chem. 63, 4699-4707.

Weir A., Westerhoff P., Fabricius L., Hristovski K. and von Goetz N. (2012). Titanium dioxide nanoparticles in food and personal care products. Environ. Sci. Technol. 46, 2242-2250.

Wen S., Li K., Cai H., Chen Q., Shen M., Huang Y., Peng C., Hou W., Zhu M., Zhang G. and Shi X. (2013). Multifunctional dendrimer-entrapped gold nanoparticles for dual mode CT/MR imaging applications. Biomaterials 34, 1570-1580.

Yu Y., Wu Y., Liu J.J., Zhan Y. and Wu D. (2016). Ultrasmall dopamine-coated nanogolds: preparation, characteristics, and CT imaging. J. Exp. Nanosci. 11, S1-S11.

Zehedina K., Nurunnabi M., Nafiujjaman M., Reeck G., Khan H.A., Cho K.J. and Lee Y. (2015). A hyaluronic acid nanogel for photo-chemo theranostic of lung cancer with simultaneous light-responsive controlled release of doxorubicin. Nanoscale 7, 10680-10689.

Zhang X.D., Wu D., Shen X., Chen J., Sun YM., Liu PX. and Liang X.J. (2012). Size-dependent radiosensitization of PEG-coated gold nanoparticles for cancer radiation therapy. Biomaterials 33, 6408-6419.

Zhang J., Nie X., Ji Y., Liu Y., Wu X., Chen C. and Fang X. (2014). Quantitative biokinetics and systemic translocation of various gold nanostructures are highly dependent on their size and shape. J. Nanosci. Nanotechnol. 14, 4124-4138.

Zhang X., Qian J. and Pan B. (2016). Fabrication of novel magnetic nanoparticles of multifunctionality for water decontamination. Environ. Sci. Technol. 50, 881-889.

Accepted September 28, 2016